Unveiling the phase diagram of a striped cuprate at high magnetic fields: Hidden order of Cooper pairs

Zhenzhong Shi,[1†] P. G. Baity,[1,2] T. Sasagawa,[3] Dragana Popović[1,2*]

[1]National High Magnetic Field Laboratory, Florida State University,
Tallahassee, Florida 32310, USA
[2]Department of Physics, Florida State University,
Tallahassee, Florida 32306, USA
[3]Materials and Structures Laboratory, Tokyo Institute of Technology,
Kanagawa 226-8503, Japan

[†] Present address: Department of Physics, Duke University,
Durham, North Carolina 27708, USA
[*]To whom correspondence should be addressed; E-mail: dragana@magnet.fsu.edu

The interplay of charge orders with superconductivity in underdoped cuprates at high magnetic fields (H) is an open question, and even the value of the upper critical field (H_{c2}), a measure of the strength of superconductivity, has been the subject of a long-term debate. We combined three complementary transport techniques on underdoped $La_{1.8-x}Eu_{0.2}Sr_xCuO_4$ with a "striped" charge order and a low $H = 0$ transition temperature T_c^0, to establish the T–H phase diagram and reveal the ground states in CuO_2 planes: a superconductor, a wide regime of superconducting phase fluctuations (i.e. a vortex liquid), and a high-field normal state. The relatively high H_{c2} is consistent with the opening of a superconducting gap

above T_c^0, but only at $T \sim$ (2-3)T_c^0, an order of magnitude below the pseudogap temperature. Within the vortex liquid, an unanticipated, insulatinglike region, but with strong superconducting correlations, begins to emerge already at $T \lesssim T_c^0$. The results suggest that the presence of stripes plays a crucial role in the freezing of Cooper pairs in this novel state. Our findings provide a fresh perspective on the pairing strength in underdoped cuprates, and introduce a new avenue for exploring the interplay of various orders.

A central issue for cuprate high-temperature superconductivity (HTSC) is the nature and the temperature evolution of superconducting correlations in the pseudogap regime of underdoped cuprates[1]. The suppression of HTSC by an external magnetic field has been one of the main methods to reveal and probe this unusual "normal" state. However, the identification of the H-induced normal state has been a challenge, because the interplay of thermal fluctuations, quantum fluctuations, and disorder generally leads to a complex T–H phase diagram of vortices or quantized magnetic flux lines penetrating the type-II superconductor[2–4]. For example, thermal and quantum fluctuations cause melting of the vortex solid, present at low fields, into a vortex liquid (VL), which may survive up to surprisingly high fields[5,6] at $T \ll T_c(H = 0) \equiv T_c^0$. Hence, for cuprates with a relatively high T_c^0, the H-induced normal state may be experimentally inaccessible. The understanding of the normal state is further complicated by the nearly ubiquitous existence of periodic modulations of charge density in superconducting cuprates[7], raising questions about the precise interplay of charge order and HTSC, especially under extreme conditions of high magnetic fields[7,8]. Therefore, the key question is the evolution of superconducting correlations with both T and H in the presence of charge order, as well as the evolution of ground states with H.

Underdoped cuprates are highly anisotropic, layered materials, and thus behave effectively as two-dimensional (2D) systems[5,9,10]. Understanding the suppression of 2D superconductivity by H and the nature of the resulting ground states remains, however, a fundamental problem in its own right even in conventional superconductors[11,12]. In particular, the key issues are the role of the vortex matter and the existence of intermediate phases. For example, in weakly disordered films (with normal state resistivity ρ_n small compared to the quantum of resistance h/e^2), anomalous metallic states have been reported (e.g. refs. 13–18), but they remain controversial and not well understood. Studies of cuprates, which are relatively clean materials, can thus provide important insight into the nature of ground states in 2D systems in the presence of H (ref. 5).

To address the above questions, we study underdoped $La_{1.8-x}Eu_{0.2}Sr_xCuO_4$ (LESCO) in which static, short-range charge order is present already at $H = 0$ and, as in other La-based cuprates[19], it coexists with the antiferromagnetic spin-density-wave order at low enough $T < T_{SO} < T_{CO}$; here T_{SO} and T_{CO} are the onsets of static, short-range spin and charge orders or "stripes", respectively, and $T_c(x)$ is suppressed for doping near $x = 1/8$ (Supplementary Fig. 1). Fields perpendicular to CuO_2 planes, i.e. along the c axis, enhance both spin[20,21] and charge orders[22,23]. These effects are observed only below T_c^0, not above, and in samples away from $x = 1/8$, such as $x \sim 0.10$, where the stripe order is weaker. The emergence and an enhancement of the charge order by H below T_c^0, accompanying the suppression of HTSC, has been observed[24] also in $YBa_2Cu_3O_{6+x}$ (YBCO). While there is no evidence of coincident static spin order in YBCO (ref. 1), it has been argued[25] that the charge order in YBCO is similar to that in La-based cuprates and, in fact, that charge-density-wave modulations persist in the $T = 0$ field-induced normal state in underdoped YBCO and in Hg- and La-based cuprates[25]. Hence, we focus on LESCO with $x = 0.10$, in which the stripe order is expected to be enhanced by $H \parallel c$

and to persist even after T_c is suppressed to zero.

By measuring both linear and nonlinear in-plane transport on single crystals with the nominal composition $La_{1.7}Eu_{0.2}Sr_{0.1}CuO_4$ (Methods), as well as the anisotropy ratio ρ_c/ρ_{ab} (here ρ_c and ρ_{ab} are the out-of-plane and in-plane resistivity, respectively), we map out the evolution of superconducting correlations with H over an unusually large, more than three-orders-of-magnitude-wide range of T down to $T/T_c^0 \lesssim 0.003$ (Methods). Most strikingly, the resulting phase diagram, sketched in Fig. 1, shows that, at $T \lesssim T_c^0$, a novel phase begins to emerge *within* a VL that separates a superconductor and a normal state: although characterized by strong superconducting correlations, this phase exhibits *insulatinglike* behavior.

In-plane resistivity of $La_{1.7}Eu_{0.2}Sr_{0.1}CuO_4$

For the in-plane transport, $T_c^0 = (5.7 \pm 0.3)$ K was defined as the temperature at which ρ_{ab} becomes zero. In $La_{1.7}Eu_{0.2}Sr_{0.1}CuO_4$, $T_{SO} \sim 15$ K, $T_{CO} \sim 40$ K (Supplementary Fig. 1), and the pseudogap temperature $T_{pseudogap} \sim 175$ K (ref. 26).

The in-plane magnetoresistance (MR) measurements show (Fig. 2a) that the positive MR, indicative of the suppression of SC, appears below ~ 35 K. As T decreases further, a negative MR develops at the highest fields, resulting in a peak in $\rho_{ab}(H)$ at $H = H_{peak}(T)$ for $T < T_c^0$. In cuprates, a peak in the MR has been observed[27] so far only in underdoped $La_{2-x}Sr_xCuO_4$ (LSCO), and its similarities to that in films of conventional superconductors near a field-tuned superconductor-insulator transition have led to the suggestion[28] that, in both cases, H_{peak} represents the field scale above which the superconducting gap, a measure of the pairing strength between electrons that form Cooper pairs, vanishes. The most interesting, novel observation though is that of a shoulder that appears in the MR in the $H < H_{peak}$ region for $T \lesssim 1$ K and becomes more pronounced with decreas-

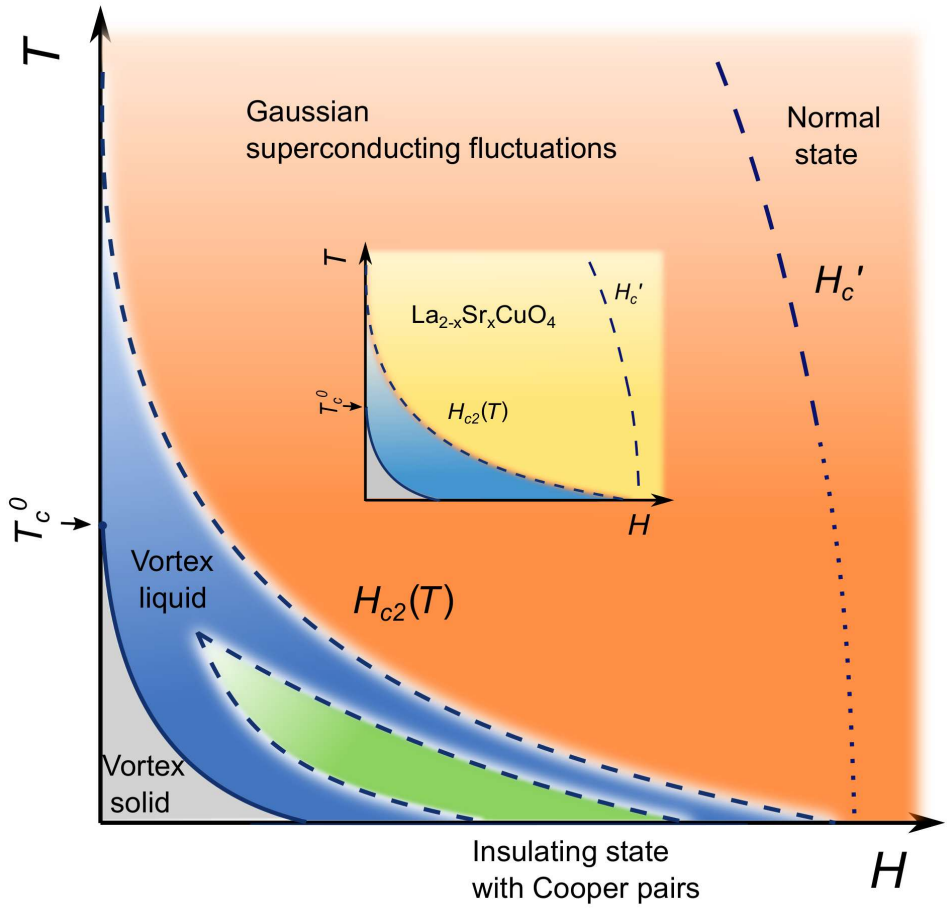

Figure 1: **Schematic T–H phase diagram of a striped LESCO.** The pinned vortex solid (Bragg glass) is a superconductor characterized by zero resistivity for all $T < T_c(H)$ (solid blue line). The vortex liquid, i.e. a vortex glass, is a superconductor with $T_c = 0$; it is bounded by the crossover line $H_{c2}(T)$. Gaussian fluctuations of the superconducting amplitude and phase are observable for $H_{c2}(T) < H < H_c'(T)$. A dotted line is obtained by extrapolating the measured high-T values of H_c' to lower T. The normal state is observed at the highest fields, as shown. A novel, insulatinglike state (green) emerges within the vortex liquid at $T \lesssim T_c^0$, but it retains strong superconducting correlations characteristic of a vortex liquid, indicating the presence of Cooper pairs. The origin of this hidden order of Cooper pairs seems to be due to the presence of stripes. For comparison, the inset shows a schematic of the T–H phase diagram of underdoped LSCO (ref. 5), where this novel regime is absent.

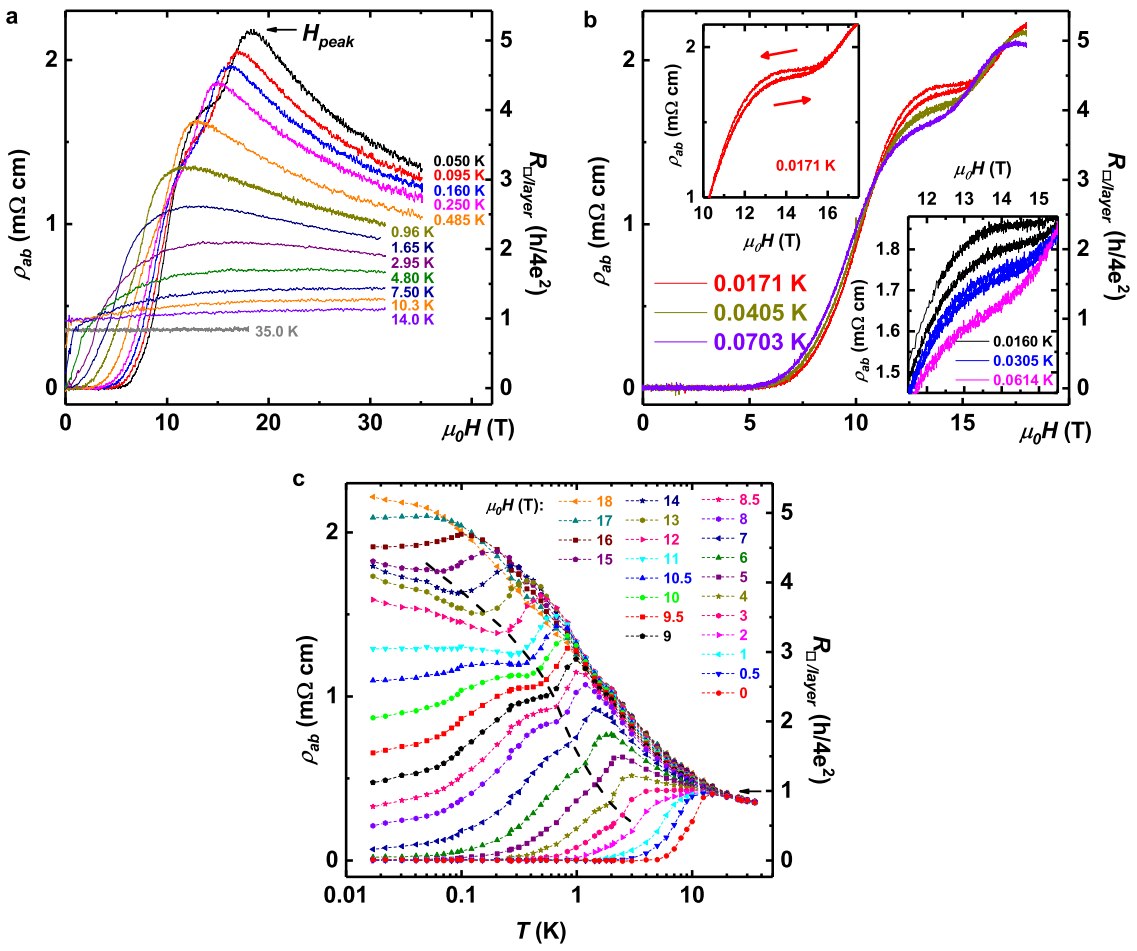

Figure 2: **The dependence of the in-plane resistivity ρ_{ab} on magnetic field $H \parallel c$ and T.** **a**, $\rho_{ab}(H)$ for several T from 0.05 K to 35.0 K, as shown. At low T, $\rho_{ab}(H)$ exhibits a strong peak at $H = H_{peak}(T)$. The right axis shows the corresponding $R_{\square/\text{layer}}$ in units of quantum resistance for Cooper pairs, $R_Q = h/(2e)^2$. **b**, In the $H < H_{peak}$ region at the lowest temperatures, $\rho_{ab}(H)$ exhibits a shoulder with the hysteretic behavior and insulatinglike T dependence. The same width of the hysteretic region was found for field sweep rates between 0.1 T/min, shown here, and 1 T/min. Arrows in the upper left inset show the direction of field sweeps. The hysteresis is suppressed with increasing T and becomes unobservable above $\sim$ 0.05 K (lower right inset). **c**, $\rho_{ab}(T)$ for $H \leq 18$ T, as shown. Short-dashed lines guide the eye. The black dashed line tracks the values of T where the metalliclike drop of $\rho_{ab}(T)$ is interrupted or weakened, turning into insulatinglike behavior at higher H. This line matches closely the values of H_b in Fig. 3. The arrow shows that the splitting of the $\rho_{ab}(T)$ curves for different H becomes pronounced when $R_{\square/\text{layer}} \approx R_Q$; $T \approx 15$ K.

ing T (Figs. 2a and 2b). At much lower $T \lesssim 0.05$ K, the MR in this range of fields becomes hysteretic, with the size of the hysteresis growing with decreasing T. Moreover, here $\rho_{ab}(T)$ has an insulatinglike T dependence (i.e. $d\rho_{ab}/dT < 0$), in contrast to the metalliclike behavior ($d\rho_{ab}/dT > 0$) outside of the hysteretic regime (Fig. 2b). In general, a hysteresis is a manifestation of the coexistence of phases, i.e. it indicates the presence of domains of different phases in the system. Typical signatures of such systems include slow, nonexponential relaxations and memory effects, which are indeed observed here, within the hysteretic regime (Supplementary Fig. 2).

Figure 2c and Supplementary Fig. 3 show the $\rho_{ab}(T)$ curves extracted from the MR measurements for $H \leq 18$ T and $18 \leq H(\mathrm{T}) \leq 35$, respectively. When the normal state sheet resistance, $R_{\square/\mathrm{layer}}$, is close to the quantum resistance for Cooper pairs, $R_Q = h/(2e)^2$, which occurs for $T \approx 15$ K, the $\rho_{ab}(T)$ curves start to separate from each other (Fig. 2c): lower-H $\rho_{ab}(T)$ curves exhibit a metalliclike drop associated with SC, while higher-H curves show a tendency towards insulating behavior. This is remarkably reminiscent of the critical resistance close to R_Q in 2D films of many materials at a $T = 0$ phase transition from a superconductor to an insulator[11,12]. Such a transition is generally attributed to the destruction of superconducting coherence by strong phase fluctuations; Cooper pairs that form the superconducting condensate thus survive the transition to the insulator. In $La_{1.7}Eu_{0.2}Sr_{0.1}CuO_4$, the low-$T$ behavior is more complicated than in this simplest scenario, with the $\rho_{ab}(T)$ curves exhibiting nonmonotonic behavior. In particular, the dashed line in Fig. 2c tracks the values of T where the metalliclike drop of $\rho_{ab}(T)$ is interrupted or weakened, starting from $T \sim 2$ K for $H \sim 3$ T, and then turning into insulatinglike behavior at higher H (e.g. $T \sim 0.3$ K for $H \sim 11$ T). This line matches closely the values of H_b in the phase diagram (Fig. 3), which were determined precisely from the enhancement of the anisotropy, as discussed below. At the highest H, $\rho_{ab}(T)$

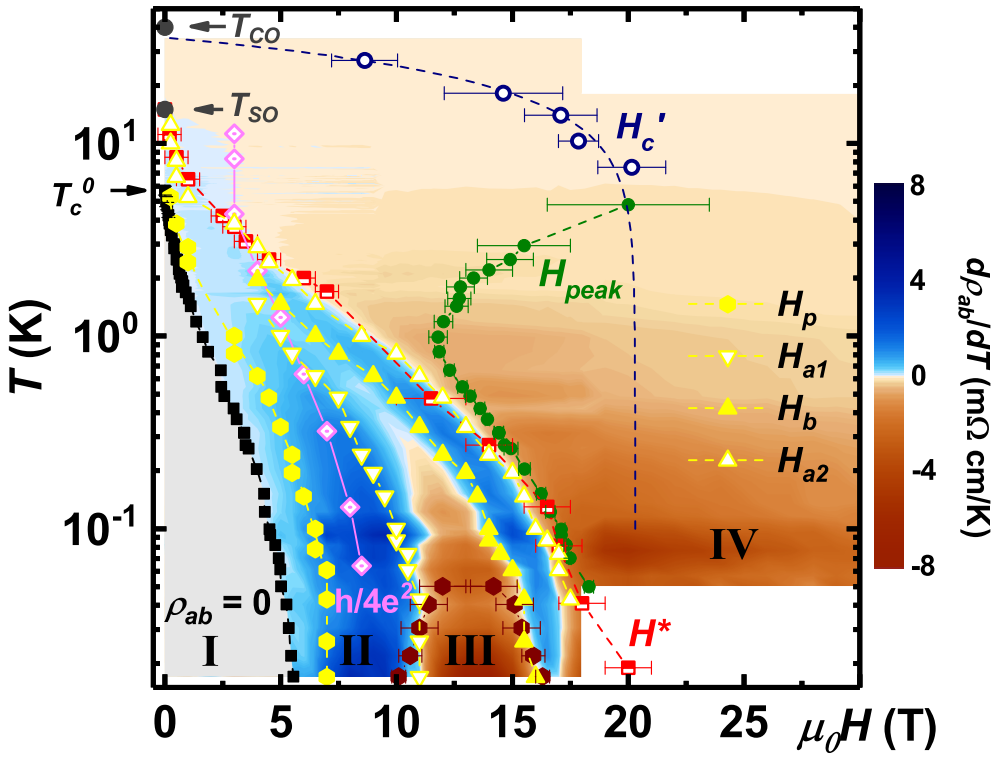

Figure 3: **In-plane transport T–H phase diagram of $La_{1.7}Eu_{0.2}Sr_{0.1}CuO_4$ with $H \parallel c$ axis.** Black squares mark $T_c(H)$, i.e. the boundary of the superconductor with $\rho_{ab} = 0$ for all $T < T_c(H)$ [region I; $T_c(H) > 0$]. $H^*(T)$ symbols, obtained from dV/dI measurements, mark the boundary of the vortex liquid, i.e. a vortex glass with $T_c = 0$, in which dV/dI is non-Ohmic [for $H < H^*(T)$]; Ohmic behavior is found at $H > H^*(T)$. The color map shows the slopes $d\rho_{ab}/dT$, clearly indicating the emergence of an insulatinglike region at $T \lesssim T_c(H = 0)$ within the vortex liquid (VL). The domelike region (III) is the (T, H) range in which the magnetoresistance (MR) hysteresis is observed; the error bars result from the uncertainty in ρ_{ab} due to T fluctuations. $H_{peak}(T)$ (green dots) represent fields above which the MR changes from positive to negative. H_c', extracted from the positive MR at high temperatures (Supplementary Fig. 6), is the field above which superconducting fluctuations are not observed; the dashed line is a fit with $\mu_0 H_c'[\mathrm{T}] = 20.3[1-(T[\mathrm{K}]/35.4)^2]$, and the error bars indicate the uncertainty in H_c' that corresponds to 1 SD in the slopes of the linear fits in Supplementary Fig. 6. The $h/4e^2$ line shows the (T, H) values where the sheet resistance, or resistance per square per CuO_2 layer, $R_{\square/\mathrm{layer}}$, changes from $R_{\square/\mathrm{layer}} < R_Q = h/4e^2$ at lower H, to $R_{\square/\mathrm{layer}} > R_Q$ at higher H. Region IV is the H-induced normal state. The fields $H_p(T)$, $H_{a1}(T)$, $H_b(T)$, and $H_{a2}(T)$ (yellow symbols) show where characteristic changes in ρ_c/ρ_{ab} occur, with $H_{a1}(T)$ and $H_b(T)$ reflecting the emergence of the novel insulatinglike region within the VL. Blank (white) areas are regions with no data available. Zero-field values of T_{SO} and T_{CO} are also shown; both spin and charge stripes are known to be enhanced by H (see main text).

exhibits the $\ln(1/T)$ dependence (Supplementary Fig. 3). Figure 3 shows $d\rho_{ab}/dT$ as a function of T and H, in addition to $T_c(H)$, H_{peak}, and the boundary of the hysteretic region.

The quantum melting of the vortex solid, in which $\rho_{ab} = 0$ as the vortices are pinned by disorder[2–4], occurs when $T_c(H) \to 0$ for $H \sim 5.5$ T. The vortex solid is surrounded by the region of metalliclike behavior ($d\rho_{ab}/dT > 0$; blue in Fig. 3), which is expected to correspond to a VL, i.e. a regime of strong phase fluctuations, in type-II superconductors such as cuprates[2–4]. Indeed, in the intermediate H regime (II in Fig. 3), the data are described best with the power-law fits $\rho_{ab}(H,T) = \rho_0(H)T^{\alpha(H)}$ (Supplementary Fig. 4), suggesting a true superconducting state ($\rho_{ab} = 0$) only at $T = 0$ when the vortices are frozen, and consistent with the expectations for a VL above its glass freezing temperature[29]. This finding is similar to that in highly underdoped LSCO ($x = 0.06, 0.07$) (ref. 5). However, in a striking contrast to LSCO, which at best has a very weak charge order[30], an unanticipated region of insulatinglike ($d\rho_{ab}/dT < 0$) behavior emerges within the phase-fluctuations regime, becoming broader with decreasing T (Fig. 3). Although it is most pronounced for $T \lesssim 0.05$ K (domelike region III) where the hysteretic phenomena are observed, the precursors, i.e. the weakening of the metalliclike T dependence, become visible already below ~ 1 K. This corresponds to the appearance of a shoulder in the MR curves (Figs. 2a and 2b). We note that the insulatinglike $d\rho_{ab}/dT$ that develops in region III is at least as strong as the one observed at the highest fields (Supplementary Fig. 5).

Interestingly, the line of (T, H) values where $R_{\square/\text{layer}}$ changes from $R_{\square/\text{layer}} < R_Q$ at lower H, to $R_{\square/\text{layer}} > R_Q$ at higher H ("$h/4e^2$" line in Fig. 3), extrapolates roughly to the lower-field end of the hysteretic dome ($H \sim 10$ T) as $T \to 0$, suggesting that the onset of the dome may be related to the localization of Cooper pairs. These observations naturally raise the question about the extent of superconducting correlations.

Nonlinear transport and superconducting correlations

The onset of superconducting fluctuations can be determined from the positive MR at high T (Fig. 2a) as the field $H'_c(T)$ above which the MR increases as H^2 (Supplementary Fig. 6), as expected in the normal state, and fitted with $H'_c = H'_0[1-(T/T_2)^2]$ (Fig. 3)[5,10,31–34]. This method, however, cannot be used at lower T where the MR develops a peak (Fig. 2a), and it is less direct than the nonlinear transport measurement. The second technique, therefore, involves measurements of nonlinear current-voltage (I–V) characteristics at fixed H and T (Methods), in addition to the linear resistance $R_{ab} \equiv \lim_{I_{dc}\to 0} V/I$ discussed above. When $T < T_c$, dV/dI is zero as expected in a superconductor (Supplementary Fig. 7a), since small values of I_{dc} are not able to cause the depinning of the vortex solid. However, at higher H, where T_c is suppressed to zero, a zero-resistance state is not observed even at $I_{dc} = 0$ (Supplementary Fig. 7a), down to the lowest T (Fig. 4a), while the I–V characteristic remains non-Ohmic and dV/dI increases with I_{dc}. This type of behavior is attributed to the motion of vortices in the presence of disorder, i.e. it is a signature of a viscous VL or a vortex glass[2–4]. Therefore, the measured I–V characteristics support the identification of the region II and the metalliclike ($d\rho_{ab}/dT > 0$) region at higher $15 \leq H(\mathrm{T}) \leq 16.5$ (Supplementary Fig. 7b) as the VL.

Surprisingly, the same nonlinear transport is observed in the insulatinglike ($d\rho_{ab}/dT < 0$) regime that emerges within this VL (Fig. 4b and Supplementary Fig. 7b). Here, the increase of dV/dI with I_{dc} is precisely the opposite of what would be expected in the case of simple Joule heating, confirming the presence of superconducting correlations in the domelike region III of the phase diagram (Fig. 3). A systematic study of nonlinear transport for different T and H (e.g. Supplementary Fig. 7c) establishes the non-Ohmic behavior for all $H < H^*(T)$ and Ohmic behavior for $H > H^*(T)$ in Fig. 3; as $T \to 0$,

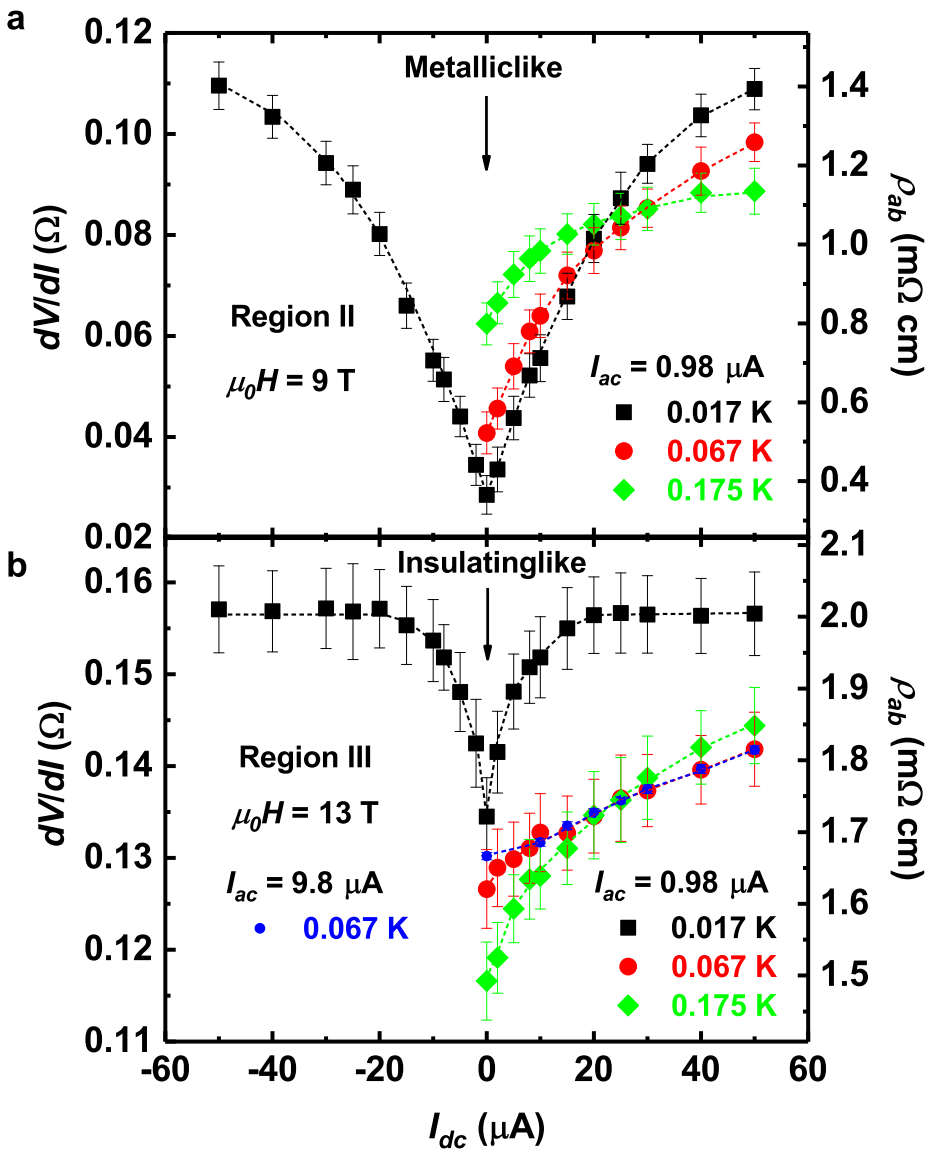

Figure 4: **Nonlinear in-plane transport.** **a** and **b**, dV/dI vs. I_{dc} for several T at $H = 9$ T and $H = 13$ T, respectively. The temperature dependence of the linear resistance (dV/dI for $I_{dc} \to 0$) is metalliclike in region II (**a**) and insulatinglike in region III (**b**). In all dV/dI measurements, $I_{ac} \approx 1$ μA, but the data taken at $T = 0.067$ K show that the same result is obtained, within the error, with $I_{ac} \approx 1$ μA and $I_{ac} \approx 10$ μA (**b**). Dashed lines guide the eye.

both H^* and H_c' extrapolate to $\sim$ 20 T. The $H < H^*(T)$ region is thus dominated by phase fluctuations, while the $H^*(T) < H < H_c'(T)$ regime is described by a vanishing superconducting gap and Gaussian fluctuations of amplitude and phase; region IV ($H > H^*, H_c'$) corresponds to the high-field-induced normal state (Supplementary Information). Previously, a much lower, $\sim$ 8 T pair-breaking field was reported on $La_{1.7}Eu_{0.2}Sr_{0.1}CuO_4$ (ref. 35), but the Cooper pair condensate with strong superconducting correlations clearly survives up to much higher $H \approx H^*$ (Fig. 3).

Anisotropy

The evidence for novel ordering of Cooper pairs comes also from the anisotropic transport (Fig. 5). In $H = 0$, ρ_c vanishes at (5.5$\pm$0.3) K (Supplementary Fig. 8), i.e. at the same T_c^0 within the error as ρ_{ab}, indicating the onset of 3D SC. This is similar to LSCO (e.g. ref. 27), but notably different from a striped $La_{2-x}Ba_xCuO_4$ with $x = 1/8$ (ref. 36), in which a 2D SC is established at a T higher than the onset of 3D SC. In Fig. 5, the anisotropy at the highest $T = 20$ K is $\rho_c/\rho_{ab} \sim 6000$ and practically independent of H. However, as T is lowered below T_c^0, ρ_c/ρ_{ab} develops a distinctly nonmonotonic behavior as a function of H. At $T = 0.017$ K, for example, the anisotropy increases with H by over an order of magnitude before reaching a peak ($\rho_c/\rho_{ab} > 10^5$) at the field H_p, followed by a similarly large decrease to H-independent values, comparable to those at high T, for the highest $H > 20$ T. This further supports our conclusion that the $H > 20$ T region corresponds to the normal state. Interestingly, a smooth, rapid decrease of the anisotropy for $H > H_p$ is interrupted by a "bump" or an enhancement in ρ_c/ρ_{ab}, occurring at H_b between the fields H_{a1} and H_{a2} (Fig. 5). These characteristic fields are strongly pronounced in the second temperature derivative even at fairly high T (Supplementary Fig. 9), which is how they were therefore determined more precisely for the in-plane phase diagram in Fig. 3.

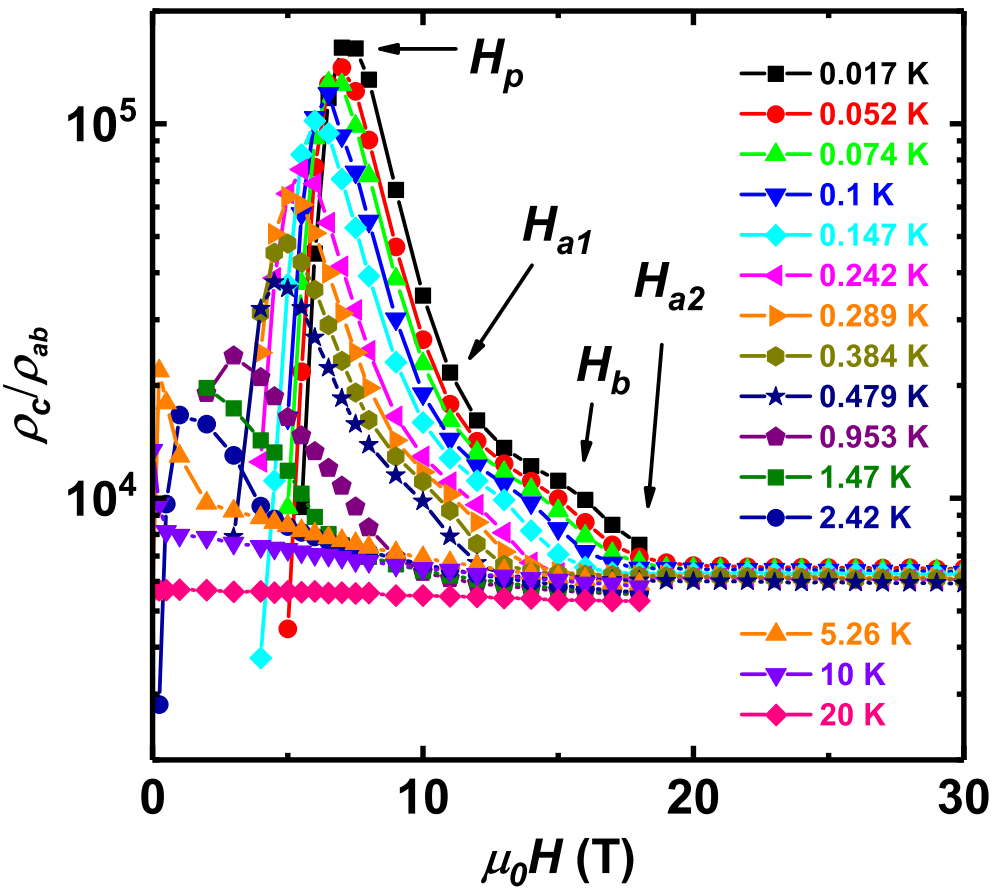

Figure 5: **Anisotropic transport for different $H \parallel c$ and T.** The anisotropy ratio ρ_c/ρ_{ab} vs. H at different T, as shown. Solid lines guide the eye. Arrows show the positions of the anisotropy peak H_p, as well as fields H_{a1}, H_{a2}, and H_b that characterize the region of a slower decrease of anisotropy with increasing field. The method to determine H_{a1}, H_{a2}, and H_b precisely is described in Fig. S9.

A huge increase in ρ_c/ρ_{ab} as H rises up to H_p at a fixed T, corresponding to the regime where both $\rho_{ab}(T)$ and $\rho_c(T)$ rapidly increase from zero (Supplementary Fig. 10), signifies decoupling of or the loss of phase coherence between CuO_2 planes. However, strong superconducting correlations persist in the planes for $H > H_p$. Evidence for layer decoupling by $H \parallel c$, while leaving in-plane SC nearly intact, was obtained also in underdoped LSCO (ref. 37) and $La_{1.905}Ba_{0.095}CuO_4$ (ref. 38). As H increases further and weakens the SC, ρ_c/ρ_{ab} decreases and reaches the normal-state background at $H_{a2} \approx H^*$ ($\sim$ 20 T as $T \to 0$). Most strikingly, the emerging insulatinglike region is bounded by fields H_{a1} and H_b (Fig. 3), thus strongly suggesting that it corresponds to some kind of a rearrangement of the superconducting order in the planes.

Summary and discussion

Upper critical field. In cuprates, the value of H_{c2}, i.e. the field above which vortices disappear and superconducting gap closes as $T \to 0$, has been of great interest, because the strength of pairing correlations is an essential ingredient in understanding what controls the value of T_c^0, the nature of the pairing mechanism, and the pseudogap regime[1]. However, the interpretation of experimental data has been controversial and contradictory (refs. 6, 26, 39, 40 and refs. therein). At least a part of the controversy lies in a disagreement on whether the VL regime vanishes[39] or persists[6] at $T = 0$. By performing both linear and nonlinear transport measurements, which are sensitive to global phase coherence, we provide a new perspective on this question.

First, since phase fluctuations in $H = 0$ dominate at $T \lesssim 15$ K $\sim$ (2-3)T_c^0 and Gaussian fluctuations of amplitude and phase become observable below T_{CO} (Fig. 3), we find no evidence for pairing at temperatures comparable to $T_{pseudogap}$, similar to the conclusions of other, recent studies[10,26]. Measurements at relatively high $T < T_c$ suggest low values

of H^* needed to close the gap (Fig. 3), consistent with some reports[26,35] of low values of H_{c2}. By extrapolating to $T \to 0$ in different families of cuprates, it was then argued[39] that there is no VL regime at $T = 0$. However, by extending our studies to $T/T_c^0 \ll 1$, our work shows clearly that the VL regime *broadens* dramatically as T is reduced: the VL thus survives up to fields $H_{c2} = H^* \sim 20$ T as $T \to 0$, i.e. well beyond the quantum melting field of the vortex solid ($\sim$ 5.5 T). The relatively high H_{c2} is consistent with the onset of phase fluctuations at $T \lesssim 15$ K in $H = 0$. We note that, at $T < 0.4$ K, $H_{peak} \approx H^*$ (Fig. 3), suggesting that, for $T \ll T_c^0$, H_{peak} may be interpreted as the field scale corresponding to the closing of the superconducting gap[28]. This implies that H_{c2} has not been reached in YBCO for any doping, since only a region of positive MR has been observed.

The similarity between our results on LESCO and low-T experiments on underdoped LSCO (ref. 5) and YBCO (ref. 6) implies that the pairing strength in underdoped cuprates is not only robust, but also not very sensitive to the details of the competing charge orders. Our data show that, in contrast, the disorder plays an important role for $H < H^*$, causing the freezing of the VL into a vortex glass phase with $T_c = 0$, in analogy with the findings on LSCO (ref. 5 and Fig. 1). The relevance of disorder as a possible solution of the controversy about H_{c2} was conjectured[40] even for YBCO, the cleanest cuprate. Indeed, we demonstrate that the disorder does play an important role as $T \to 0$, and show that extreme conditions of very low $T/T_c^0 < 10^{-2}$ and probes sensitive to vortex matter, such as nonlinear I–V, are crucial for identifying the states in the quantum limit in the cuprates. This is consistent with theoretical expectations that, at low T, the effects of disorder on the vortex matter become increasingly important as H increases[4].

Evolution of ground states with H. By mapping out the evolution of superconducting correlations over an uncommonly large range of T and H, we have also revealed for the

first time a full sequence of ground states in a striped cuprate (Fig. 1): a low-H, pinned vortex solid phase with $T_c(H) > 0$ ("Bragg glass"[4]), a higher-H vortex glass phase with $T_c = 0$, and a high-field normal state; the latter tends to a metal for $H \gtrsim 55$ T (Supplementary Information). In general, the two superconducting ground states with different ordering of the vortex matter can form only when the disorder is relatively weak[4]. Indeed, in $La_{1.7}Eu_{0.2}Sr_{0.1}CuO_4$, $\rho_n < h/e^2$ (see, e.g., highest T in Fig. 2c) and, even in highly underdoped LSCO, $\rho_n \lesssim h/e^2$ (ref. 5). For $H > H_p$ (Fig. 3), $La_{1.7}Eu_{0.2}Sr_{0.1}CuO_4$ behaves as a 2D system and exhibits several similarities to thin films of conventional superconductors. However, the emergence of the insulatinglike phase within the VL (Fig. 3), but with strong superconducting correlations characteristic of a VL (i.e. an increase of dV/dI with I_{dc}, as shown in Fig. 4), is unprecedented: it does not resemble anything that has been reported in other 2D superconductors. Namely, an increase of dV/dI with I_{dc} has been observed[13] only in the *metallic* state that separates a weakly disordered 2D superconductor from the higher-field insulatinglike state in which dV/dI *decreases* with I_{dc}. This, together with the absence of an insulatinglike regime within the VL in highly underdoped LSCO (ref. 5 and Fig. 1), suggests that the origin of the novel insulatinglike behavior with the VL-like I–V characteristic (Fig. 4b) in $La_{1.7}Eu_{0.2}Sr_{0.1}CuO_4$ may be related to the presence of stripes.

Origin of the novel state of Cooper pairs. Important insight can be gained by noting some similarities in the behavior of ρ_c/ρ_{ab} as the superconducting state is approached from the normal state in $La_{1.7}Eu_{0.2}Sr_{0.1}CuO_4$, by reducing H at $T \to 0$ (Fig. 3), and in $La_{1.875}Ba_{0.125}CuO_4$, by lowering T in $H = 0$ (ref. 36). To explain a large increase in ρ_c/ρ_{ab} in $La_{1.875}Ba_{0.125}CuO_4$, it was proposed that the in-plane SC takes the form of a pair density wave (PDW)[41,42], in which SC is spatially modulated so that it occurs most strongly within the charge stripes, but the phases between adjacent stripes are reversed

(antiphase). Since stripes are rotated by 90° from one layer to next, antiphase SC within a plane strongly suppresses the c-axis Josephson coupling and thus 3D SC[19], leading to an increase in anisotropy. This effect is reduced[41] by the presence of disorder and doping away from $x = 1/8$, which could account for the observation of a 3D SC in $La_{1.7}Eu_{0.2}Sr_{0.1}CuO_4$ for $H < H_p$, but not in $La_{1.875}Ba_{0.125}CuO_4$. In the PDW scenario, the effective Josephson coupling between neighboring charge stripes in each plane is mediated by the antiphase antiferromagnetic order of spin stripes[41,42] that lie between charge stripes at $T < T_{SO}$. The onset of the phase-fluctuations-dominated regime below T_{SO} (Fig. 3) is consistent with this picture.

Therefore, within the PDW scenario, the appearance of the insulatinglike state between the fields H_{a1} and H_b (Fig. 3) might correspond to the suppression of Josephson coupling between neighboring stripes with increasing H: when Josephson coupling between charge stripes is destroyed by H, Cooper pairs are confined to the quasi-1D regions, resulting in an enhancement of the anisotropy (by a factor of ~ 2 at the lowest T, with respect to the monotonically decreasing component; Fig. 5). This picture is also consistent with $R_{\Box/\mathrm{layer}} > R_Q$ at $H \sim H_{a1}$ as $T \to 0$ that suggests the localization of Cooper pairs in this region. A PDW of localized pairs without global phase coherence has been proposed[43] as the dominant competing order in the pseudogap state ($T > T_c^0$ and $H = 0$). We note that the precursors, H_{a1} and H_b, of the novel insulatinglike state become visible at a fairly high $T \sim 2$ K and relatively low $H \sim 5$ T when $R_{\Box/\mathrm{layer}} \gtrsim R_Q$ (Fig. 3), suggesting that this state is indeed close in energy to the fluctuating 2D SC that develops in region II for $H > H_p$. It is thus possible to speculate that region III might represent a coexistence of the usual, spatially uniform SC and a PDW SC. Such a state would not be sensitive to disorder[44], and it could also account for the intriguing reentrance of the VL for $H_b < H < H_{a2} \approx H^*$. The weak insulatinglike behavior in region III would arise

from the localization into some form of a Wigner crystal of Cooper pairs[45,46], consistent with the expectation of weak, as opposed to strong, insulatinglike T dependence above the melting temperature of the Wigner crystal, which may be very low[47,48].

Alternatively, it might be tempting to attribute the insulatinglike behavior in region III to the properties of the normal state, i.e. region III could represent a coexistence of the VL and the normal state. However, this cannot account for the reentrance of the VL for $H_b < H < H_{a2} \approx H^*$. One might also speculate that the emergence of region III with the hysteretic MR is related to some kind of a H-induced phase transition occurring in the stripe system itself, in particular spin stripes. Indeed, our observations are somewhat reminiscent of the novel phase of $Sr_3Ru_2O_7$ that forms in the vicinity of a metamagnetic quantum critical point[49] and results from H-tuned transitions between spin-density-wave phases[50]. Although no evidence suggestive of such a transition has been reported in underdoped cuprates, this regime of very low T and high H has not been explored. Therefore, just like in $Sr_3Ru_2O_7$, other experiments will be needed to unravel the origin of the novel state and the precise nature of the hidden order of Cooper pairs in LESCO.

Conclusion. The quantitative agreement of the results obtained from three different, complementary techniques on a striped LESCO with low T_c^0 has allowed us to map out the $T - H$ phase diagram over more than three orders of magnitude of T and deep into the H-induced normal state. Our results establish the importance of vortex matter physics and disorder as $T \to 0$ in underdoped cuprates, providing a fresh perspective on the long-standing question about the strength of pairing correlations in the pseudogap regime. In addition, we have discovered a novel type of insulatinglike regime, but with strong superconducting correlations characteristic of a VL and emergence *within* a VL. The presence of stripes seems to play a crucial role in the freezing of Cooper pairs in this

novel state. The identification of such an unconventional and unanticipated state, albeit not inconsistent with some theoretical scenarios, paves the way for experimental studies also in other underdoped cuprates, to gain further insight into the nature of HTSC and its interplay with other orders in cuprates.

Methods

Samples. Several single crystal samples of $La_{1.8-x}Eu_{0.2}Sr_xCuO_4$ (Supplementary Fig. 1) with a nominal $x = 0.10$, grown by the traveling-solvent floating-zone technique[51], were shaped as rectangular bars suitable for direct measurements of the in-plane and out-of-plane resistance. Detailed measurements were performed on two crystals with dimensions $3.06\times0.37\times0.53$ mm^3 and $0.34\times0.41\times1.67$ mm^3 ($a\times b\times c$). Gold contacts were evaporated on polished crystal surfaces, and annealed in air at 700 °C. The current contacts were made by covering the whole area of the two opposing sides with gold to ensure uniform current flow, and the voltage contacts were made narrow to minimize the uncertainty in the absolute values of the resistance. The distance between the voltage contacts is 1.53 mm for the in-plane sample, and 0.47 mm for the out-of-plane sample. Gold leads (≈ 25 μm thick) were attached to the samples using the Dupont 6838 silver paste, followed by the heat treatment at 450 °C in the flow of oxygen for 15 minutes. The resulting contact resistances were less than 0.1 Ω at room temperature.

Measurements. The standard four-probe ac method ($\sim$ 13 Hz) was used for measurements of the sample resistance, with the excitation current (density) of 10 μA ($\sim 5\times10^{-3}$ A cm^{-2}) for the in-plane sample and 10 nA ($\sim 7\times10^{-6}$ A cm^{-2}) for the out-of-plane sample. dV/dI measurements were performed by applying a dc current bias (density) down to 2 μA ($\sim 1\times10^{-3}$ A cm^{-2}) and a small ac current excitation $I_{ac} \approx 1$ μA

($\sim$ 13 Hz) through the sample and measuring the ac voltage across the sample. For each value of I_{dc}, the ac voltage was monitored for 300 s and the average value recorded. The relaxations of dV/dI with time, similar to that in Fig. S2A, were observed only at the lowest $T \sim 0.016$ K. Even then, the change of dV/dI during the relaxation, reflected in the error bars for the $T = 0.017$ K data in Fig. 4, was much smaller than the change of dV/dI with I_{dc}. The data that were affected by Joule heating at large dc bias were not considered. In the high-field normal state, for example, the dc current bias where Joule heating becomes relevant, identified as the current above which the I-V characteristic changes from Ohmic to non-Ohmic, was $I_{dc} > 100$ μA at the lowest T. In all measurements, a π filter was connected at the room temperature end of the cryostat to provide a 5 dB (60 dB) noise reduction at 10 MHz (1 GHz).

The experiments were conducted in several different magnets at the National High Magnetic Field Laboratory: a dilution refrigerator (0.016 K $\leqslant$ T $\leqslant$ 0.7 K) and a ^{3}He system (0.3 K $\leqslant$ T $\leqslant$ 35 K) in superconducting magnets (H up to 18 T), using 0.1 – 0.2 T/min sweep rates; a portable dilution refrigerator (0.02 K $\leqslant$ T $\leqslant$ 0.7 K) in a 35 T resistive magnet, using 1 T/min sweep rate; and a ^{3}He system (0.3 K $\leqslant$ T $\leqslant$ 20 K) in a 31 T resistive magnet, using 1 – 2 T/min sweep rates. Below $\sim$ 0.06 K, it was not possible to achieve sufficient cooling of the electronic degrees of freedom to the bath temperature, a common difficulty with electrical measurements in the mK range. This results in a slight weakening of the $\rho_{ab}(T)$ curves below $\sim$ 0.06 K for *all* fields. We note that this does not make any qualitative difference to the phase diagram (e.g. Fig. 3). The fields, applied perpendicular to the CuO_2 planes, were swept at constant temperatures. The sweep rates were low enough to avoid eddy current heating of the samples.

The resistance per square per CuO_2 layer $R_{\Box/\mathrm{layer}} = \rho/l$, where $l = 6.6$ Å is the

thickness of each layer.

Data availability. The data that support the findings of this study are available from the corresponding author upon reasonable request.

References

1. Keimer, B., Kivelson, S. A., Norman, M. R., Uchida, S. & Zaanen, J. From quantum matter to high-temperature superconductivity in copper oxides. *Nature* **518**, 179–186 (2015).

2. Blatter, G., Feigel'man, M. V., Geshkenbein, V. B., Larkin, A. I. & Vinokur, V. M. Vortices in high-temperature superconductors. *Rev. Mod. Phys.* **66**, 1125–1388 (1994).

3. Rosenstein, B. & Li, D. Ginzburg-Landau theory of type II superconductors in magnetic field. *Rev. Mod. Phys.* **82**, 109–168 (2010).

4. Le Doussal, P. Novel phases of vortices in superconductors. *Int. J. Mod. Phys. B* **24**, 3855-3914 (2010).

5. Shi, X., Lin, P. V., Sasagawa, T., Dobrosavljević, V. & Popović, D. Two-stage magnetic-field-tuned superconductor-insulator transition in underdoped $La_{2-x}Sr_xCuO_4$. *Nature Phys.* **10**, 437–443 (2014).

6. Yu, F. *et al.* Magnetic phase diagram of underdoped $YBa_2Cu_3O_y$ inferred from torque magnetization and thermal conductivity. *Proc. Natl. Acad. Sci. USA* **113**, 12667–12672 (2016).

7. Comin, R. & Damascelli, A. Resonant X-ray scattering studies of charge order in cuprates. *Annu. Rev. Condens. Matter Phys.* **7**, 369–405 (2016).

8. Julien, M.-H. Magnetic fields make waves in cuprates. *Science* **350**, 914–915 (2015).

9. Emery, V. J. & Kivelson, S. A. Importance of phase fluctuations in superconductors with small superfluid density. *Nature* **374**, 434–437 (1995).

10. Baity, P. G., Shi, X., Shi, Z., Benfatto, L. & Popović, D. Effective two-dimensional thickness for the Berezinskii-Kosterlitz-Thouless-like transition in a highly underdoped $La_{2-x}Sr_xCuO_4$. *Phys. Rev. B* **93**, 024519 (2016).

11. Goldman, A. M. Supeconductor-insulator transitions. *Int. J. Mod. Phys.* **24**, 4081–4101 (2010).

12. Gantmakher, V. F. & Dolgopolov, V. T. Superconductor-insulator quantum phase transition. *Physics-Uspekhi* **53**, 1–49 (2010).

13. Qin, Y., Vicente, C. L. & Yoon, J. Magnetically induced metallic phase in superconducting tantalum films. *Phys. Rev. B* **73**, 100505(R) (2006).

14. Steiner, M. A., Breznay, N. P. & Kapitulnik, A. Approach to a superconductor-to-Bose-insulator transition in disordered films. *Phys. Rev. B* **77**, 212501 (2008).

15. Saito, Y., Kasahara, Y., Ye, J., Iwasa, Y. & Nojima, T. Metallic ground state in an ion-gated two-dimensional superconductor. *Science* **350**, 409–413 (2015).

16. Tsen, A. W. *et al.* Nature of the quantum metal in a two-dimensional crystalline superconductor. *Nature Phys.* **12**, 208 (2016).

17. Breznay, N. P., Tendulkar, M., Zhang, L., Lee, S.-C. & Kapitulnik, A. Superconductor to weak-insulator transitions in disordered tantalum nitride films. *Phys. Rev. B* **96**, 134522 (2017).

18. Breznay, N. P. & Kapitulnik, A. Particle-hole symmetry reveals failed superconductivity in the metallic phase of two-dimensional superconducting films. *Science Advances* **3**, e1700612 (2017).

19. Fradkin, E., Kivelson, S. A. & Tranquada, J. M. Colloquium: Theory of intertwined orders in high temperature superconductors. *Rev. Mod. Phys.* **87**, 561–563 (2015).

20. Lake, B. *et al.* Antiferromagnetic order induced by an applied magnetic field in a high-temperature superconductor. *Nature* **415**, 299–302 (2002).

21. Chang, J. *et al.* Tuning competing orders in $La_{2-x}Sr_xCuO_4$ cuprate superconductors by the application of an external magnetic field. *Phys. Rev. B* **78**, 104525 (2008).

22. Wen, J. *et al.* Uniaxial linear resistivity of superconducting $La_{1.905}Ba_{0.095}CuO_4$ induced by an external magnetic field. *Phys. Rev. B* **85**, 134513 (2012).

23. Hücker, M. *et al.* Enhanced charge stripe order of superconducting $La_{2-x}Ba_xCuO_4$ in a magnetic field. *Phys. Rev. B* **87**, 014501 (2013).

24. Gerber, S. *et al.* Three-dimensional charge density wave order in $YBa_2Cu_3O_{6.67}$ at high magnetic fields. *Science* **350**, 949–952 (2015).

25. Badoux, S. *et al.* Critical doping for the onset of Fermi-surface reconstruction by charge-density-wave order in the cuprate superconductor $La_{2-x}Sr_xCuO_4$. *Phys. Rev. X*, 021004 (2016).

26. Cyr-Choinière, O. *et al.* Pseudogap temperature T^* of cuprate superconductors from the Nernst effect. Preprint at http://arxiv.org/abs/1703.06927 (2017).

27. Ando, Y., Boebinger, G. S., Passner, A., Kimura, T. & Kishio, K. Logarithmic divergence of both in-plane and out-of-plane normal-state resistivities of superconducting $La_{2-x}Sr_xCuO_4$ in the zero-temperature limit. *Phys. Rev. Lett.* **75**, 4662–4665 (1995).

28. Steiner, M. A., Boebinger, G. & Kapitulnik, A. Possible field-tuned superconductor-insulator transition in high-T_c superconductors: Implications for pairing at high magnetic fields. *Phys. Rev. Lett.* **94**, 107008 (2005).

29. Dorsey, A. T., Huang, M. & Fisher, M. P. A. Dynamics of the normal to vortex-glass transition: Mean-field theory and fluctuations. *Phys. Rev. B* **45**, 523–526 (1992).

30. Jacobsen, H. *et al.* Neutron scattering study of spin ordering and stripe pinning in superconducting $La_{1.93}Sr_{0.07}CuO_4$. *Phys. Rev. B* **92**, 174525 (2015).

31. Rullier-Albenque, F. *et al.* Total suppression of superconductivity by high magnetic fields in $YBa_2Cu_3O_{6.6}$. *Phys. Rev. Lett.* **99**, 027003 (2007).

32. Rullier-Albenque, F., Alloul, H. & Rikken, G. High-field studies of superconducting fluctuations in high-T_c cuprates: Evidence for a small gap distinct from the large pseudogap. *Phys. Rev. B* **84**, 014522 (2011).

33. Rourke, P. M. C. *et al.* Phase-fluctuating superconductivity in overdoped $La_{2-x}Sr_xCuO_4$. *Nature Phys.* **7**, 455–458 (2011).

34. Shi, X. *et al.* Emergence of superconductivity from the dynamically heterogeneous insulating state in $La_{2-x}Sr_xCuO_4$. *Nature Mater.* **12**, 47–51 (2013).

35. Chang, J. *et al.* Decrease of upper critical field with underdoping in cuprate superconductors. *Nature Phys.* **8**, 751–756 (2012).

36. Li, Q., Hücker, M., Gu, G. D., Tsvelik, A. M. & Tranquada, J. M. Two-dimensional superconducting fluctuations in stripe-ordered $La_{1.875}Ba_{0.125}CuO_4$. *Phys. Rev. Lett.* **99**, 067001 (2007).

37. Schafgans, A. A. *et al.* Towards a two-dimensional superconducting state of $La_{2-x}Sr_xCuO_4$ in a moderate external magnetic field. *Phys. Rev. Lett.* **104**, 157002 (2010).

38. Stegen, Z. *et al.* Evolution of superconducting correlations within magnetic-field-decoupled $La_{2-x}Ba_xCuO_4$ ($x = 0.095$). *Phys. Rev. B* **87**, 064509 (2013).

39. Grissonnanche, G. *et al.* Direct measurement of the upper critical field in cuprate superconductors. *Nature Commun.* **5**, 3280 (2014).

40. Zhou, R. *et al.* Spin susceptibility of charge ordered $YBa_2Cu_3O_y$ across the upper critical field. *PNAS* **114**, 13148–13153 (2017).

41. Berg, E. *et al.* Dynamical layer decoupling in a stripe-ordered high-T_c superconductor. *Phys. Rev. Lett.* **99**, 127003 (2007).

42. Himeda, A., Kato, T. & Ogata, M. Stripe states with spatially oscillating d-wave superconductivity in the two-dimensional t-t'-J model. *Phys. Rev. Lett.* **88**, 117001 (2002).

43. Chen, H.-D., Vafek, O., Yazdani, A. & Zhang, S.-C. Pair density wave in the pseudogap state of high temperature superconductors. *Phys. Rev. Lett.* **93**, 187002 (2004).

44. Berg, E., Fradkin, E., Kivelson, S. A. & Tranquada, J. M. Striped superconductors: how spin, charge and superconducting orders intertwine in the cuprates. *New J. Phys.* **11**, 115004 (2009).

45. Chen, H.-D., Hu, J.-P., Capponi, S., Arrigoni, E. & Zhang, S.-C. Antiferromagnetism and hole pair checkerboard in the vortex state of high T_c superconductors. *Phys. Rev. Lett.* **89**, 137004 (2002).

46. Rastelli, G., Quémerais, P. & Fratini, S. Enhancement of Wigner crystallization in quasi-low-dimensional solids. *Phys. Rev. B* **73**, 155103 (2006).

47. Huang, J., Novikov, D. S., Tsui, D. C., Pfeiffer, L. N. & West, K. W. Nonactivated transport of strongly interacting two-dimensional holes in GaAs. *Phys. Rev. B* **74**, 201302(R) (2006).

48. Pramudya, Y., Terletska, H., Pankov, S., Manousakis, E. & Dobrosavljević, V. Nearly frozen Coulomb liquids. *Phys. Rev. B* **84**, 125120 (2011).

49. Grigera, S. A. *et al.* Disorder-sensitive phase formation linked to metamagnetic quantum criticality. *Science* **306**, 1154–1157 (2004).

50. Lester, C. *et al.* Field-tunable spin-density-wave phases in $Sr_3Ru_2O_7$. *Nature Mater.* **14**, 373–378 (2015).

51. N. Takeshita, T. Sasagawa, T. Sugioka, Y. Tokura, H. Takagi, Gigantic anisotropic uniaxial pressure effect on superconductivity within the CuO_2 plane of $La_{1.64}Eu_{0.2}Sr_{0.16}CuO_4$: Strain control of stripe criticality. *J. Phys. Soc. Jpn.* **73**, 1123–1126 (2004).

Acknowledgements

We acknowledge helpful discussions with V. Dobrosavljević, S. A. Kivelson, J. M. Tranquada, and J. Zaanen. This work was supported by NSF Grants Nos. DMR-1307075 and DMR-1707785, and the National High Magnetic Field Laboratory (NHMFL) through the NSF Cooperative Agreement No. DMR-1157490 and the State of Florida.

Author contributions

Z.S. and D.P. conceived the project; single crystals were grown and prepared by T.S.; Z.S. and P.G.B. performed the measurements; Z.S. analysed the data; D.P. contributed to the data analysis and interpretation; Z.S. and D.P. wrote the manuscript; D.P. planned and supervised the investigation. All authors commented on the manuscript.

Additional information

Supplementary information accompanies this paper. Correspondence and requests for materials should be addressed to D.P. (email: dragana@magnet.fsu.edu).

Competing financial interests

The authors declare no competing financial interests.

Supplementary Information

High-field normal state

Since all of the results provide evidence for the absence of SC for $H > 20$ T, they strongly suggest that region IV in Fig. 1 ($H > H^*, H'_c$) corresponds to the high-field-induced normal state. In this regime, $\rho_{ab} \propto \ln(1/T)$ over a temperature range of one-and-a-half decades, without any sign of saturation down to at least ~ 0.06 K or $T/T_c^0 \sim 10^{-2}$ (Fig. S3). The $\ln(1/T)$ behavior was first reported in underdoped $La_{2-x}Sr_xCuO_4$ [S4], but its origin is still not well understood [S5]. Nevertheless, experiments suggest that the high-field normal-state in underdoped $La_{2-x}Sr_xCuO_4$ is an insulator [S4–S6]. In contrast, a clear weakening of the insulatinglike, $\ln(1/T)$ behavior with H is observed in $La_{1.7}Eu_{0.2}Sr_{0.1}CuO_4$ (Fig. S3), strongly suggesting that ρ_{ab} becomes independent of T, i.e. metallic, at much higher fields $\gtrsim 55$ T (Fig. S3 inset). We note that the possibility that Gaussian fluctuations of amplitude and phase persist beyond $H^* \sim 20$ T as $T \to 0$ cannot be completely ruled out, as $H'_c(T)$ may acquire a "tail" at low T such that the fitted $H'_0 < H'_c(T = 0)$ [S5]. Therefore, it would be interesting to perform additional studies of the normal state in the $\ln(1/T)$ regime, as well as to extend the measurements to $H > 55$ T to probe the properties of the high-field metal phase.

Supplementary Information References

[S1] Autore, M. *et al.* Phase diagram and optical conductivity of $La_{1.8-x}Eu_{0.2}Sr_xCuO_4$. *Phys. Rev. B* **90**, 035102 (2014).

[S2] Klauss, H.-H. *et al.* From antiferromagnetic order to static magnetic stripes: The phase diagram of $(La, Eu)_{2-x}Sr_xCuO_4$. *Phys. Rev. Lett.* **85**, 4590–4593 (2000).

[S3] Fink, J. *et al.* Phase diagram of charge order in $La_{1.8-x}Eu_{0.2}Sr_xCuO_4$ from resonant soft x-ray diffraction. *Phys. Rev. B* **83**, 092503 (2011).

[S4] Ando, Y., Boebinger, G. S., Passner, A., Kimura, T. & Kishio, K. Logarithmic divergence of both in-plane and out-of-plane normal-state resistivities of superconducting $La_{2-x}Sr_xCuO_4$ in the zero-temperature limit. *Phys. Rev. Lett.* **75**, 4662–4665 (1995).

[S5] Shi, X., Lin, P. V., Sasagawa, T., Dobrosavljević, V. & Popović, D. Two-stage magnetic-field-tuned superconductor-insulator transition in underdoped $La_{2-x}Sr_xCuO_4$. *Nature Phys.* **10**, 437–443 (2014).

[S6] Karpińska, K. *et al.* Magnetic-field induced superconductor-insulator transition in the $La_{2-x}Sr_xCuO_4$ system. *Phys. Rev. Lett.* **77**, 3033-3036 (1996).

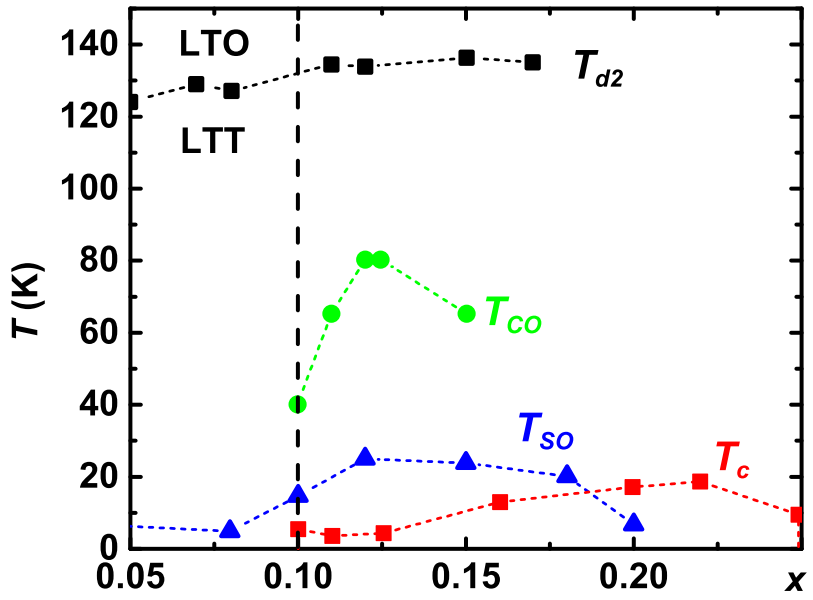

Figure S1: ***T*–*x* phase diagram of $La_{2-x}Eu_{0.2}Sr_xCuO_4$ for $H = 0$.** Data are reproduced from refs. [S1-S3]. T_{d2} marks the transition temperature from the low-temperature orthorhombic (LTO) structure to a low-temperature tetragonal (LTT) structure. T_{CO} and T_{SO} are the onset temperatures for charge and spin orders, respectively. T_c is the superconducting transition temperature. Dotted lines guide the eye. The vertical dashed line shows the doping $x = 0.10$ of our single crystals.

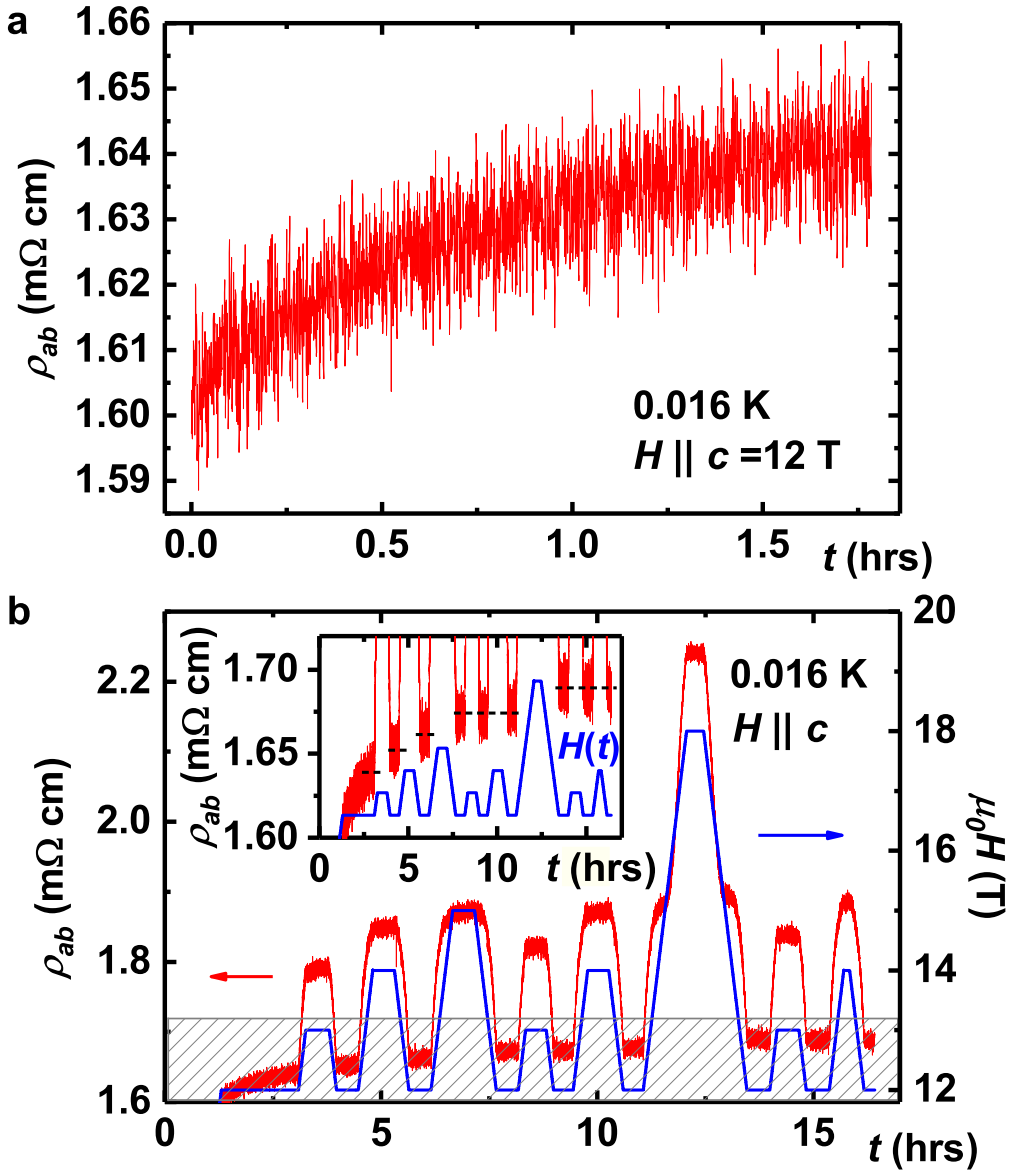

Figure S2: **Nonequilibrium dynamics in region III of the phase diagram in Fig. 3. a,** ρ_{ab} exhibits slow, nonexponential relaxations with time t: here it continues to relax for hours after the magnetic field reaches 12 T at $T = 0.016$ K. **b,** At a fixed $T = 0.016$ K, ρ_{ab} (red; left axis) is measured as a function of time as H is changed between 12 T and different higher fields (blue; right axis). This protocol allows a comparison of ρ_{ab} values obtained at the same $\mu_0 H = 12$ T but with a different magnetic history. Inset: Enlarged shaded area of the main plot shows that $\rho_{ab}(\mu_0 H = 12$ T) is determined by the highest H applied previously: the system acquires a memory of its magnetic history. Dashed lines guide the eye.

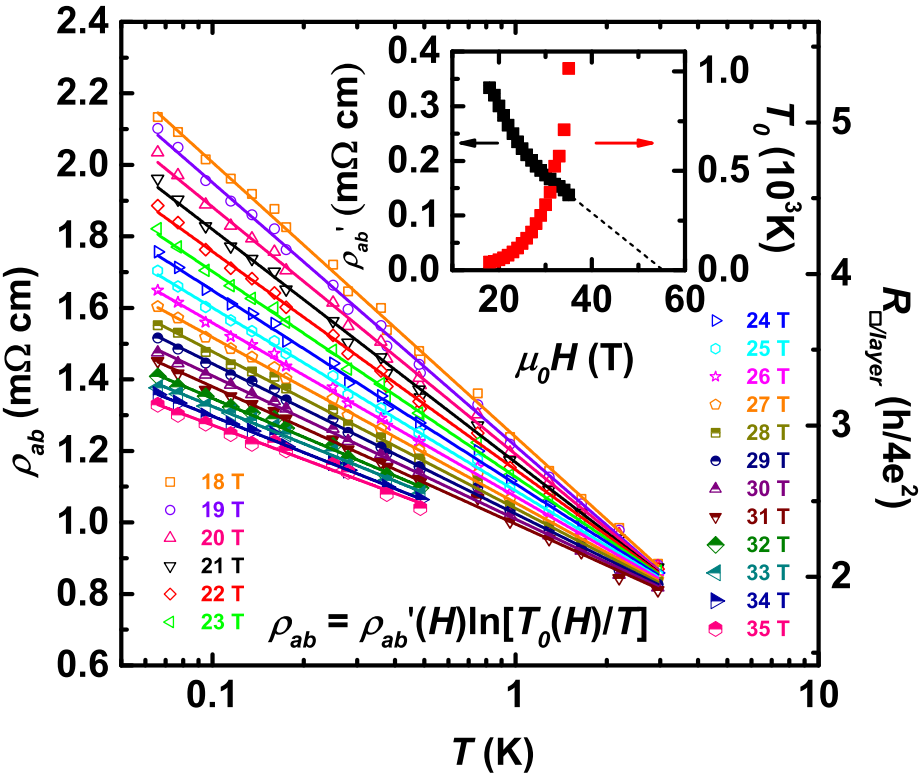

Figure S3: **The dependence of the in-plane resistivity ρ_{ab} on magnetic field $H \geq 18$ T ($H \parallel c$) and T.** $\rho_{ab}(T)$ for $18 \leq H(\mathrm{T}) \leq 35$. Solid lines are fits to $\rho_{ab} = \rho'_{ab} \ln(T_0/T)$. Inset: Fitting parameters $\rho_{ab}(H)$ and $T_0(H)$. The decrease of the slopes ρ'_{ab} with H indicates the weakening of the insulatinglike, $\ln(1/T)$ dependence with H. The linear extrapolation of ρ'_{ab} to zero (dashed line) provides a rough estimate of the field ~ 55 T where insulatinglike behavior vanishes.

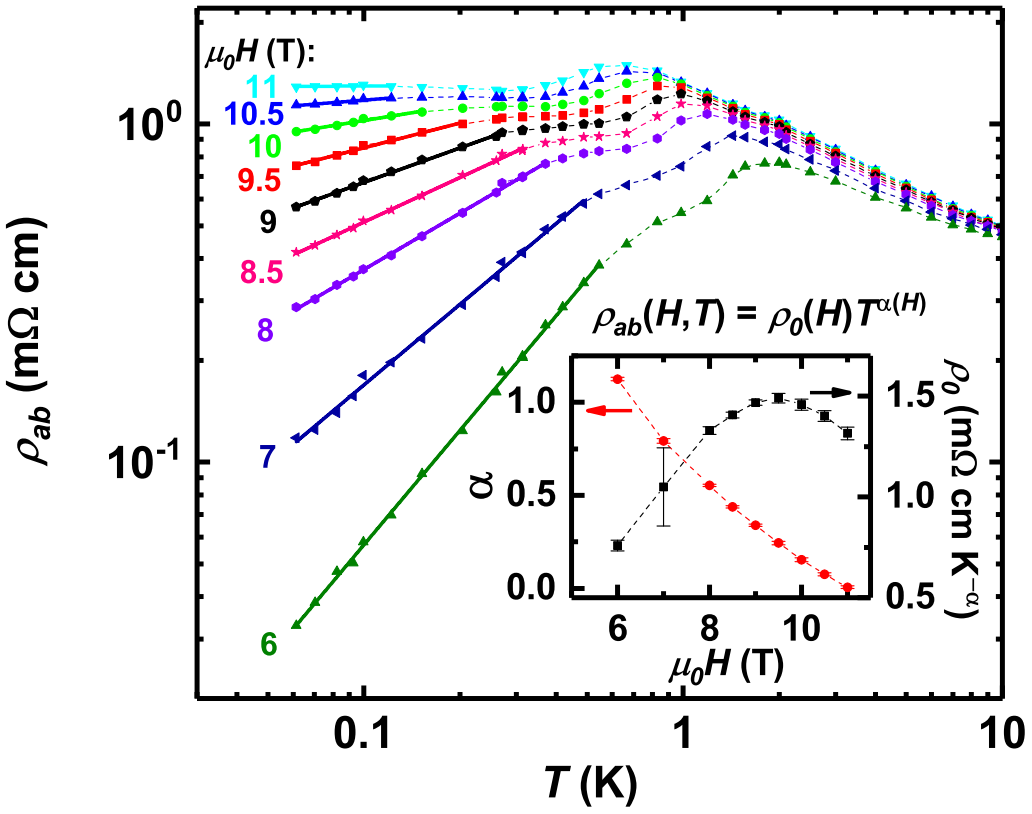

Figure S4: **The dependence of the in-plane resistivity on T at intermediate fields (region II in Fig. 3).** $\rho_{ab}(T)$ for a given H, as shown, is plotted on a log-log scale. Short-dashed lines guide the eye. Solid lines represent power-law fits $\rho_{ab}(H,T) = \rho_0(H)T^{\alpha(H)}$. Inset: Fitting parameters $\alpha(H)$ and $\rho_0(H)$. Short-dashed lines guide the eye. The linear resistance $R_{ab} \equiv \lim_{I_{dc}\to 0} V/I$ was measured with $I_{ac} \approx 10$ μA.

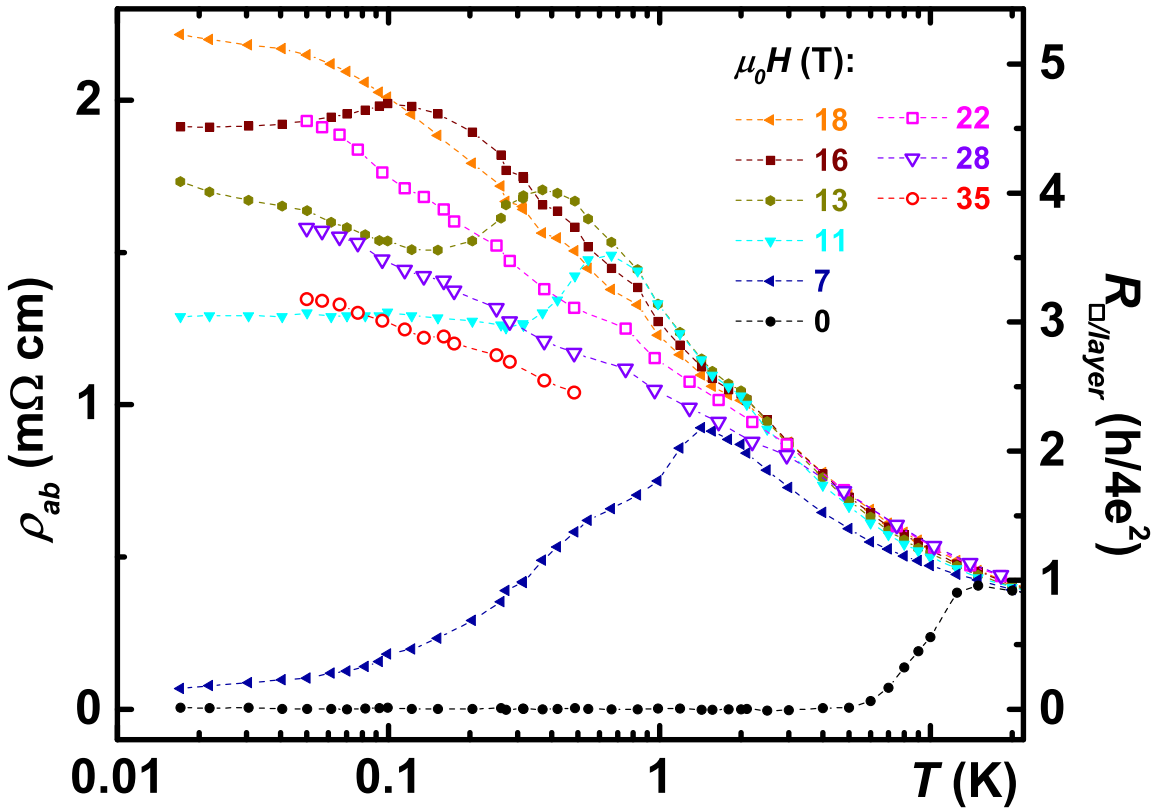

Figure S5: **The dependence of the in-plane resistivity ρ_{ab} on T for several $0 \leq H \leq 35$ T.** Dashed lines guide the eye. The insulatinglike $d\rho_{ab}/dT$ in the novel phase (region III in Fig. 3), e.g. for $H = 13$ T and $T < 0.1$ K, is comparable to that observed in the normal state ($H > 20$ T), e.g. for $H = 28$ T and $H = 35$ T.

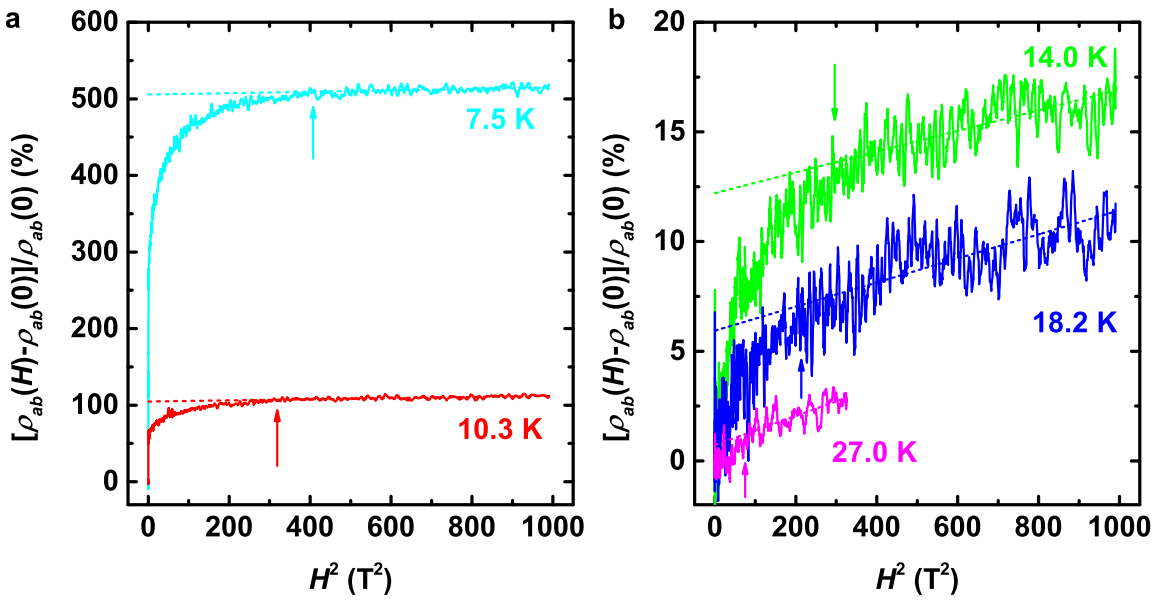

Figure S6: **In-plane magnetoresistance vs. H^2 for several $T > T_c(H = 0)$; $H \parallel c$.** In **a** and **b**, dotted lines are fits representing the contributions from normal state transport, i.e. they correspond to $[\rho_{ab}(H) - \rho_{ab}(0)]/\rho_{ab}(0) = \{[\rho_{ab}(0)]_n - \rho_{ab}(0)\}/\rho_{ab}(0) + \alpha H^2$. The intercept of the dotted line shows the relative difference between the fitted normal state resistance and the measured resistance at zero field. The difference between the dotted lines and the measured magnetoresistance is due to the superconducting contribution. Arrows indicate H_c', the field below which superconducting fluctuations become observable.

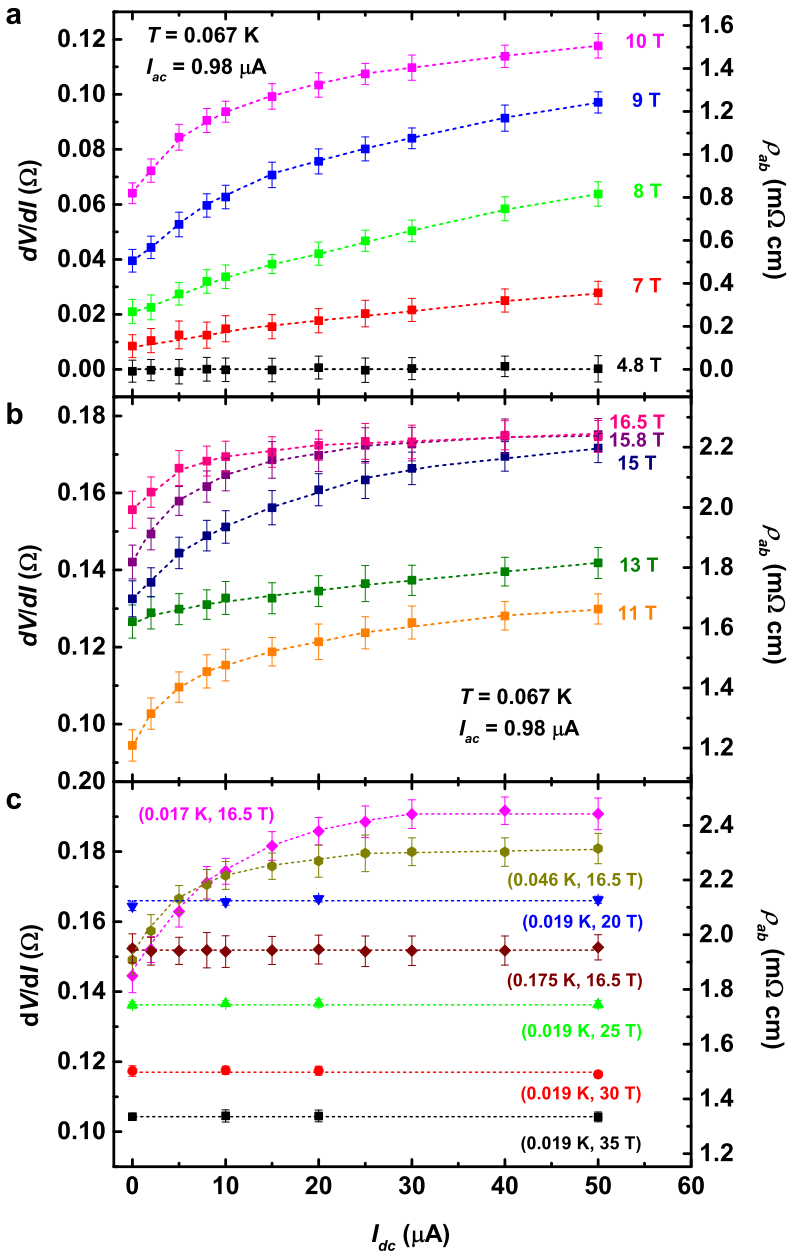

Figure S7: **Nonlinear in-plane transport.** **a,** Differential resistance dV/dI as a function of dc current I_{dc} for several $H \leq 10$ T at $T = 0.067$ K. In the bottom trace, for which $T < T_c(H = 4.8\ \mathrm{T}) \approx 0.08$ K, dV/dI is zero as expected in a superconductor. **b,** dV/dI vs. I_{dc} for several $H \geq 11$ T at $T = 0.067$ K. **c,** dV/dI vs. I_{dc} for several T and H, as shown. The data for $H = 16.5$ T were taken with $I_{ac} \approx 1\ \mu$A; for $20 \leq H(\mathrm{T}) \leq 35$, $I_{ac} \approx 10\ \mu$A. In (**a**), (**b**), and (**c**), dashed lines guide the eye.

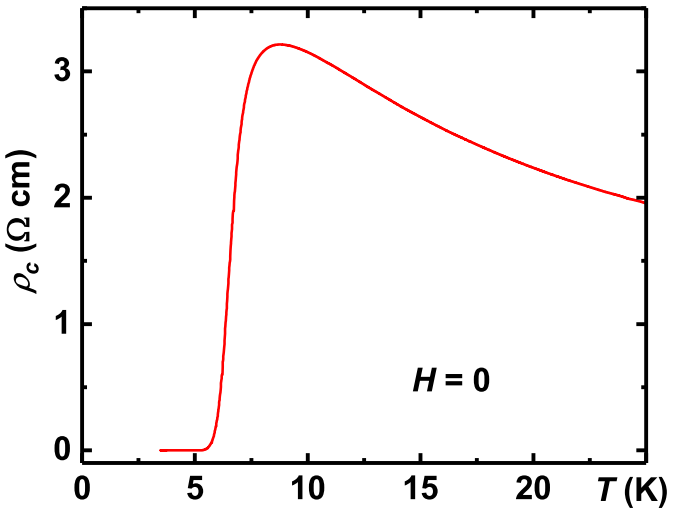

Figure S8: **Out-of-plane resistivity ρ_c vs. temperature for $H = 0$.** ρ_c drops to zero at (5.5 ± 0.3) K.

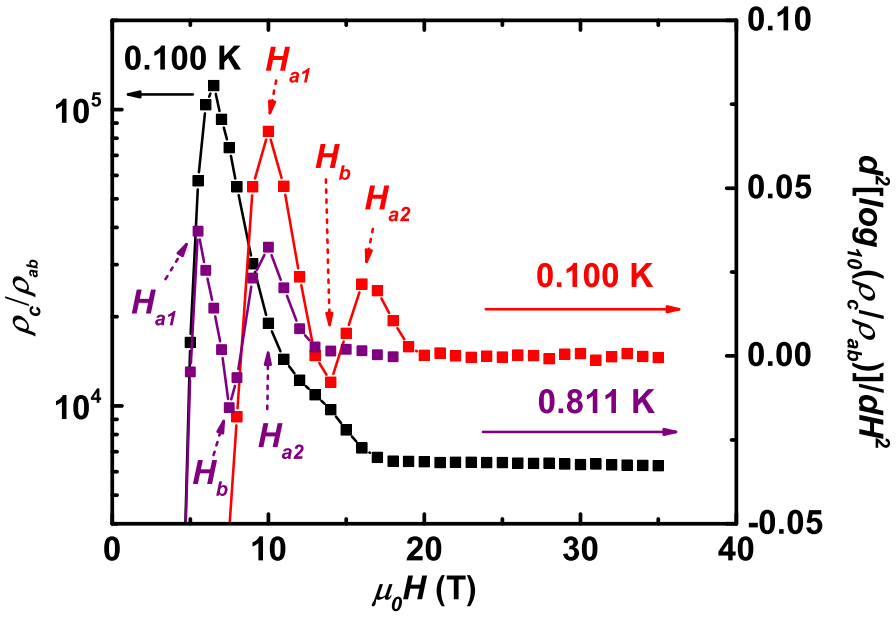

Figure S9: **Method to determine characteristic fields in the H dependence of the anisotropy ratio ρ_c/ρ_{ab}.** The anisotropy ratio ρ_c/ρ_{ab} (black symbols, left axis) vs. H at $T = 0.100$ K on a semi-log scale. Red and purple symbols (right axis) show the second derivative $d^2[\log(\rho_c/\rho_{ab})]/dH^2$ for $T = 0.100$ K and $T = 0.811$ K, respectively. Solid lines guide the eye. The fields H_{a1} and H_{a2} are defined as the maxima, and H_b as the minimum in the second derivative, as shown. Clearly, these characteristic fields remain strongly pronounced even at a fairly high T. The analysis was repeated for different T.

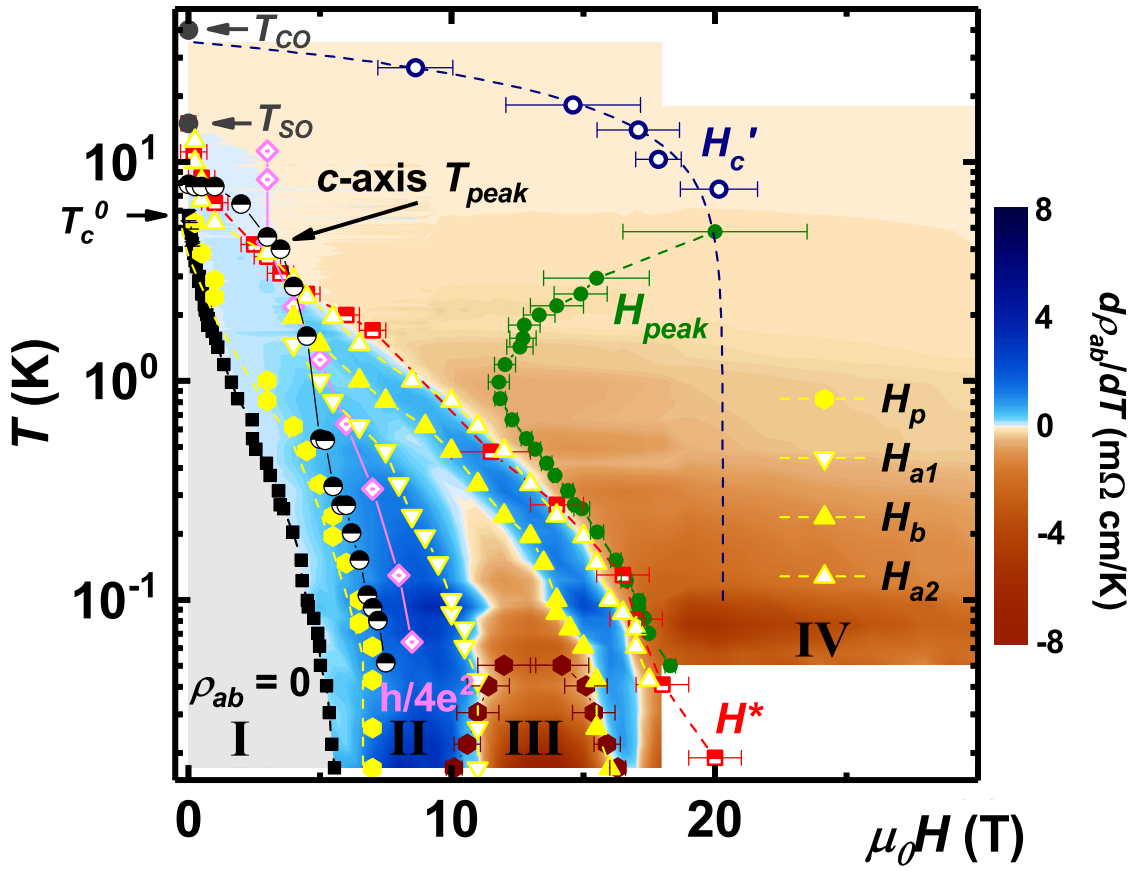

Figure S10: **In-plane transport T–H phase diagram of $La_{1.7}Eu_{0.2}Sr_{0.1}CuO_4$ with $H \parallel c$ axis.** The phase diagram from Fig. 3, with the addition of symbols denoted as "c-axis T_{peak}" that correspond to the maxima in $\rho_c(T)$ for a given field. Those symbols indicate that, for $T < T_{peak}(H)$, $d\rho_c/dT > 0$, while $d\rho_c/dT < 0$ for $T > T_{peak}(H)$. At $T \lesssim 0.5$ K, $d\rho_c/dT < 0$ for $H > H_p$.